Process-Accessible States of Block Copolymers

De-Wen Sun and Marcus Müller*
Institut für Theoretische Physik, Georg-August-Universität Göttingen, Friedrich-Hund-Platz 1, D 37077 Göttingen, Germany
(Received 17 November 2016; published 8 February 2017)

Process-directed self-assembly of block copolymers refers to thermodynamic processes that reproducibly direct the kinetics of structure formation from a starting, unstable state into a selected, metastable mesostructure. We investigate the kinetics of self-assembly of linear *ACB* triblock copolymers after a rapid transformation of the middle *C* block from *B* to *A*. This prototypical process (e.g., photochemical transformation) converts the initial, equilibrium mesophase of the *ABB* copolymer into a well-defined but unstable, starting state of the *AAB* copolymer. The spontaneous structure formation that ensues from this unstable state becomes trapped in a metastable mesostructure, and we systematically explore which metastable mesostructures can be fabricated by varying the block copolymer composition of the initial and final states. In addition to the equilibrium mesophases of linear *AB* diblock copolymers, this diagram of process-accessible states includes 7 metastable periodic mesostructures, *inter alia*, Schoen's F-RD periodic minimal surface. Generally, we observe that the final, metastable mesostructure of the *AAB* copolymer possesses the same symmetry as the initial, equilibrium mesophase of the *ABB* copolymer.

DOI: 10.1103/PhysRevLett.118.067801

The spontaneous formation of periodically ordered mesostructures with characteristic dimensions of 5–100 nm is the most characteristic and fascinating ability of block copolymers [1–3]. The stability of these self-assembled mesostructures is governed by a subtle balance of the interfacial tension between different domains and conformational stretching entropy [4]. For the deceptively simple, linear *AB* diblock copolymer melt, six spatially modulated mesophases, including close-packed spheres (cps) [5], body-centered-cubic spheres (bcc), hexagonally packed cylinders (hex), cubic gyroid networks (GYR), orthorhombic *Fddd* networks (O^{70}), and lamellae (LAM), are thermodynamically stable, equilibrium states as a function of the volume fraction, f_A, of *A* segments and the incompatibility, $\chi_{AB}N$ [4,6–8].

The free-energy landscape of diblock copolymers, however, is even more complex and features a multitude of metastable free-energy minima, e.g., alternate periodic mesostructures such as the hexagonally perforated lamellae (HPL) [1], grain boundaries, and localized defects [9]. In fact, the free-energy landscape has been likened to that of glass formers [10]. Although these mesostructures are only metastable, the free-energy barriers that separate them typically scale like $\sqrt{\bar{N}}k_{\mathrm{B}}T$ [11,12]. Thus, a large invariant degree of polymerization, $\bar{N}$, results in protracted lifetimes of minutes or hours, which suffice to additionally stabilize the mesostructures by cooling below the glass-transition temperature or cross-linking. In spite of the ubiquitous occurrence of metastable mesostructures in the course of self-assembly and the abiding interest in equilibrium mesophases and metastable mesostructures [13–18], the *kinetic pathways* that lead to the formation of desired, nonequilibrium mesostructures are rather less explored [19–21].

In this Letter, we systematically investigate a prototypical class of thermodynamic processes that start from an equilibrium mesophase and reproducibly prepare a well-defined, unstable, starting state. We design the processes so that the spontaneous structure formation that ensues from this so-prepared, starting, unstable state becomes finally trapped into a selected, metastable state and devise a diagram of process-accessible mesostructures. This diagram provides valuable insights into the complex free-energy landscape of these soft-matter systems and, potentially, enables the reproducible fabrication of novel mesostructures without the need to synthesize new complex chain architectures.

As a first exploratory step, we investigate a simple thermodynamic process: we consider an incompressible melt of linear *ACB* triblock copolymers, where the chemophysical properties of the middle block, *C*, can be rapidly altered. At the beginning, the *C* block is miscible with the *B* block and, for simplicity, we set $\chi_{BC} = 0$ and $\chi_{AB} = \chi_{AC} > 0$. Thus, the initial state is an equilibrium mesophase of the *ABB* system. Then the process renders the *C* block thermodynamically compatible with the *A* block and, specifically, we set $\chi_{AB} = \chi_{BC} > 0$ and $\chi_{AC} = 0$. In addition, we assume that the conversion of the *C* block is fast compared to the structural relaxation of the chain conformations. Such an alchemical transformation of the *C* block from *B* to *A* could potentially be realized e.g., by a photochemical reaction [22]. Whereas this specific thermodynamic process certainly is highly idealized, it is well suited to illustrate the concept of process-directed self-assembly and its potential for fabricating novel mesostructures, and to devise general correlations between the initial, equilibrium mesophase of the *ABB* system and the final,

 © 2017 American Physical Society

metastable mesostructure of the AAB system after the process.

In the following, we consider $\chi_{AB}N = 23$, where N denotes the total number of segments of a polymer, and assume that all segments are characterized by the same statistical segment length, b. All length scales are measured in units of the unperturbed polymer's end-to-end distance, $R_{e0} = b\sqrt{N}$. Since the thermodynamic process is rapid, we assume that the chain conformations remain unaltered during conversions; i.e., the initial chain conformations in the equilibrium mesophase are also characteristic of the chain conformations in the starting, unstable state. Thus, the process is specified by two parameters—the initial volume fraction of A segments, f_A, in the equilibrium mesophase and the final volume fraction of A segments, $f_A^* = f_A + f_C$,—which we systematically vary to explore the accessible metastable mesostructures.

The kinetics of structure formation is studied by dynamic self-consistent field theory (DSCFT) [26–32] using the standard Gaussian chain model [33–36], and we verify the results by single-chain-in-mean-field (SCMF) simulations [37–40] for selected parameters. The initial state—an equilibrium mesophase of a diblock copolymer with f_A—is readily obtained by static self-consistent field theory (SCFT). As we vary f_A, we obtain the equilibrium densities, $\phi_A^{\text{init}}(\mathbf{r})$ and $\phi_B^{\text{init}}(\mathbf{r}) = 1 - \phi_A^{\text{init}}(\mathbf{r})$, of the fcc, bcc, hex, GYR, and LAM mesophases with their corresponding optimal periodicities, L^{init}.

Using these equilibrium results, we calculate the density, $\tilde{\phi}_C(\mathbf{r})$, of the middle C block that corresponds to the B segments at positions, $f_A < s \le f_A^*$, where $0 \le s \le 1$ denotes the contour parameter along the chain [41]. The densities of the starting, unstable state with f_A^* after the conversion of the C block from B to A are $\phi_A^{\text{start}}(\mathbf{r}) = \phi_A^{\text{init}}(\mathbf{r}) + \tilde{\phi}_C(\mathbf{r})$ and $\phi_B^{\text{start}}(\mathbf{r}) = \phi_B^{\text{init}}(\mathbf{r}) - \tilde{\phi}_C(\mathbf{r})$, respectively, and their conjugated potential fields, $\omega_A^{\text{start}}(\mathbf{r})$ and $\omega_B^{\text{start}}(\mathbf{r})$, can be iteratively obtained. In this nonequilibrium situation, the chemical potentials, $\mu_A^{\text{start}}(\mathbf{r}) = \chi_{AB}N[\phi_B^{\text{start}}(\mathbf{r}) - f_B^*] + [\omega_B^{\text{start}}(\mathbf{r}) - \omega_A^{\text{start}}(\mathbf{r})]/2$ with $f_B^* = 1 - f_A^*$ and similarly for $\mu_B^{\text{start}}(\mathbf{r})$, vary in space and their gradients drive the kinetics of structure formation.

We employ the DSCFT to calculate the time evolution of the densities from this starting, unstable state using the optimal periodicity of the corresponding initial, equilibrium mesophase. Thus, the periodicity of the final, (meta)stable mesostructure might not coincide with its preferred periodicity, but this setting corresponds to the process of an alchemical transformation without volume change. We consider both, Allen-Cahn dynamics (model A) and Cahn-Hilliard dynamics (model B) [42]. Further details on the numerical implementations are compiled in the Supplemental Material [43]. The latter scheme, model B, locally conserves the density and thereby, mimics the underlying diffusive dynamics of polymers. In contrast to our previous study [20], however, the difference between nonconserved and conserved dynamics has almost no influence on the final observed mesostructure.

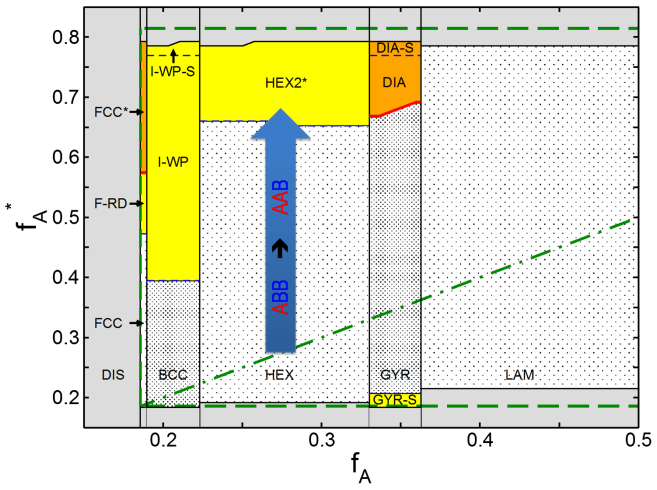

FIG. 1. Diagram of process-accessible states at $\chi_{AB}N = 23$ that is obtained by the alchemical transformation. f_A denotes the A volume fraction of the initial, equilibrium mesophase, whereas f_A^* is the A volume fraction after the alchemical conversion process. The three-letter abbreviations indicate the distinct, final mesostructures that are depicted in Fig. 2.

Since our DSCFT calculations do not include thermal noise, the process-directed self-assembly is completely deterministic, and the kinetics of structure formation becomes trapped in the first state that the system encounters in the course of the structure evolution. The results of process-directed self-assembly are compiled in the diagram of process-accessible states, Fig. 1, that presents all the final mesostructures as a function of f_A and f_A^* [50].

The diagonal, $f_A^* = f_A$, of this diagram, which is indicated by the green, dashed-dotted line in Fig. 1, corresponds to no conversion process because the length of the middle C block vanishes. Therefore, the initial and final states are identical, and both are equilibrium mesophases. The five perpendicular, black, solid lines in Fig. 1 signal to the composition, f_A, of the equilibrium phase transitions of first order between the disordered (DIS) melt, and the ordered equilibrium mesophases, fcc [51], bcc, hex, GYR, and LAM, respectively [4]. This dictates the symmetry of the initial, equilibrium mesophases. The two horizontal, green, dashed lines correspond to the final f_A^*, at which the disordered melt corresponds to the absolute minimum of the free energy.

If the C block is short, i.e., $|f_A^* - f_A| \ll 1$, the starting, unstable state that is prepared by the alchemical transformation remains in the same basin of attraction on the free-energy landscape as the initial, equilibrium mesophase. Consider, e.g., the case $f_A = \frac{28}{128}$, which corresponds to a bcc equilibrium mesophase as illustrated in Fig. 2(c). For $\frac{28}{128} < f_A^* \le \frac{50}{128}$, the final mesostructure also consists of

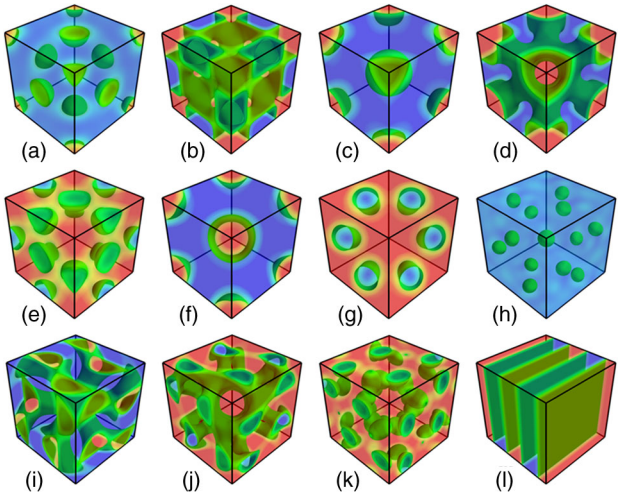

FIG. 2. Graphical representations of final mesostructures—(a) fcc, (b) F-RD, (c) bcc, (d) I-WP, (e) I-WP-S, (f) hex, (g) hex2*, (h) GYR-S, (i) GYR, (j) DIA, (k) DIA-S, (l) LAM—that can be fabricated by process-directed self-assembly using an alchemical conversion of the middle C block.

large(r), spherical A domains that are arranged on a bcc lattice. In the interval $0.189535 < f_A^* < 0.222959$, this bcc mesostructure still corresponds to the equilibrium mesophase, whereas for large f_A^* the hex, GYR, or LAM mesophase, respectively, represents the absolute minimum of the free-energy landscape.

Upon increasing f_A^* further, the character of the final, metastable mesostructure gradually changes because the A density between the enlarged A spheres increases and makes the A spheres become connected. Joining the A spheres between the first nearest neighbors results in the formation of the metastable I-WP mesostructure that is depicted in Fig. 2(d). We emphasize that this change of the final, metastable mesostructure from bcc to I-WP upon the increase of f_A^* is completely gradual, and it is not associated with a change between free-energy basins; merely, the character of the basin smoothly varies with f_A^*. Thus, bcc and I-WP are not thermodynamically different mesostructures and the location of the smooth crossover is indicated by a horizontal, blue, dashed line in this diagram.

Upon increasing f_A^* still further, i.e., for $f_A^* \geq \frac{99}{128}$, the B domains gradually break up into spheres, and the metastable I-WP-S mesostructure, which is presented in Fig. 2(e), is fabricated. Note that the alchemical conversion process does not result in a change of the basin on the free-energy landscape for all these values of f_A^*. This feature also explains why the final, metastable mesostructure is insensitive to the details of the DSCFT.

Only for $f_A = \frac{28}{128} \rightarrow f_A^* \geq \frac{102}{128}$ does the alchemical conversion process result in a basin change; in this case, the final, metastable mesostructure is the disordered state, and the concomitant transition is marked by a horizontal, black, solid line in this diagram. Note that in the interval $\frac{102}{128} \leq f_A^* < 0.814387$, the disordered state is only metastable; the thermodynamic equilibrium mesophases are bcc and fcc mesostructures, respectively, depending on the value of f_A^*.

In addition to the known thermodynamic equilibrium mesophases, the diagram of process-accessible states, Fig. 1, comprises seven additional metastable mesostructures: there are three bicontinuous network mesostructures, Schoen's F-RD [52,53], Schoen's I-WP [52,54], and the cubic single-DIAmond network (DIA) [55], as well as the graphenelike arrangement of cylindrical domains in the hex2* mesostructure [56] and different arrangements of spherical domains, I-WP-S, GYR-S, and DIA-S. This diagram also contains a fcc* mesostructure where the B block forms the spherical domains that arrange on a fcc lattice (see in the Supplemental Material [43]), which is shifted with respect to the fcc lattice of the initial, equilibrium mesophase shown in Fig. 2(a).

To the best of our knowledge, the metastable F-RD [57], I-WP-S, GYR-S, and DIA-S [58] mesostructures have not yet been experimentally observed.

Generally, the alchemical conversion process does not result in a change of free-energy basin and, consequently, the final, metastable mesostructure at f_A^* possesses the same symmetry as the initial, equilibrium mesophase at f_A. Thus, the sequence of final, metastable mesostructures upon varying f_A^* markedly differs from the sequence of equilibrium mesophases. For example, the alchemical conversion processes of the initial, equilibrium mesophase at $f_A = \frac{28}{128}$ yield the sequence of bcc, I-WP, I-WP-S, and DIS mesostructures upon increasing f_A^*, whereas the corresponding equilibrium mesophases are bcc, hex, GYR, LAM, GYR, hex, bcc, fcc, and DIS [4].

Notable exceptions from this general observation are alchemical transformations of long C blocks, i.e., large $|f_A^* - f_A|$, which catapult the starting, unstable state out of the free-energy basin of the initial, equilibrium mesophase. The new basin can be the basin of the DIS mesostructure or the basin of another spatially modulated mesostructure. There are two examples of the latter: the process-directed self-assembly from the initial, equilibrium GYR mesophase to the final, metastable DIA mesostructure and from the initial, equilibrium fcc mesophase to the final, metastable fcc* mesostructure. In the following, we focus on the case of the metastable DIA mesostructure. The case of the metastable fcc* mesostructure is discussed in the Supplemental Material [43].

To validate the DSCFT calculations, we perform SCMF simulations of a soft, particle-based model with $N = 32$ coarse-grained segments per macromolecule. The softness allows us to represent a large invariant degree of polymerization, $\sqrt{\bar{N}} = 128000$. For $f_A = \frac{11}{32}$, we equilibrate an equilibrium gyroid network in a cubic simulation cell of linear dimension $11.979 R_{e0}$ with periodic boundary

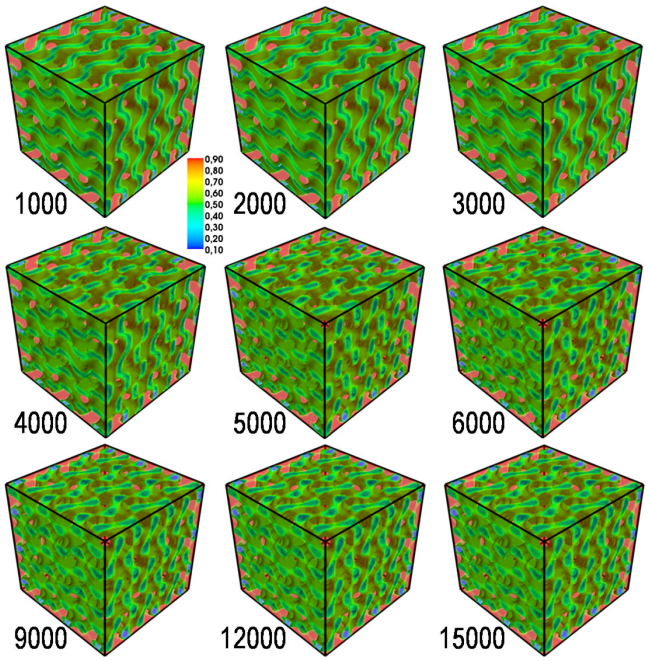

FIG. 3. Time evolution observed by SCMF simulations after an alchemical conversion process of an equilibrium gyroid network from $f_A = \frac{11}{32}$ to $f_A^* = \frac{22}{32}$ at $\chi_{AB}N = 23$. The different panels show the A density (red color) at different times measured in units of Monte Carlo (MC) steps per segment. The simulation cell totally comprises 27 cubic unit cells.

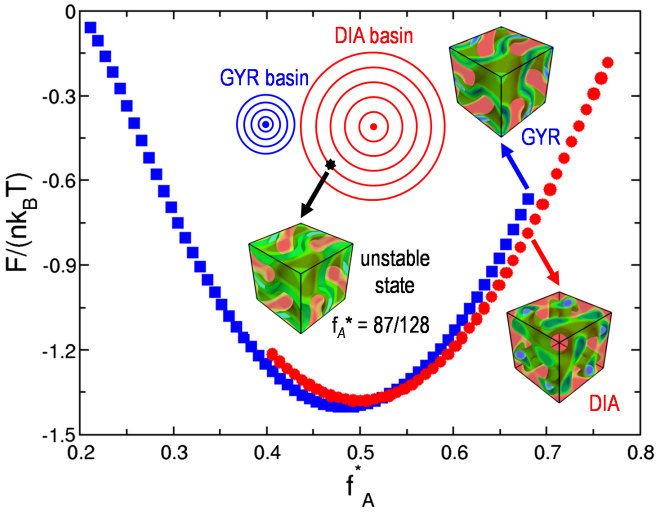

FIG. 4. Free energies of GYR and DIA mesostructures as a function of f_A^* at $\chi_{AB}N = 23$. The inset depicts the metastable GYR and DIA mesostructures at $f_A^* = \frac{87}{128}$ as well as the starting, unstable state obtained by the alchemical conversion process. The location of the starting, unstable state on the free-energy landscape is qualitatively sketched.

conditions. At frozen chain conformations, we switch the A volume fraction to $f_A^* = \frac{22}{32}$ by converting the identity of the 11 middle segments from B to A. The spontaneous structure formation from this starting, unstable state is shown in Fig. 3. First, around 1000 MC steps, we observe the formation of an A-gyroid network, which subsequently transforms into the DIA mesostructure of B channels around 5000 MC steps, which approximately correspond to half of the time a polymer chain in a disordered melt needs to diffuse a distance R_{e0}. The system only evolves slowly during the simulation runs that has been extended up to 15000 MC steps, indicating the metastability of the DIA mesostructure. A similar time evolution is also observed in both, nonconserved and conserved, DSCFT calculations.

To further illustrate the process-directed self-assembly of the metastable DIA mesostructure by an alchemical conversion process, we present in Fig. 4, the free energies of the GYR and DIA mesostructures as a function of f_A^*. In the interval $\frac{52}{128} \leq f_A^* \leq \frac{87}{128}$, both GYR and DIA mesostructures are metastable at the periodicity, $L^{\text{init}} = 3.993R_{e0}$ that is dictated by the value of the initial, equilibrium GYR mesophase at $f_A = \frac{44}{128}$. For $f_A^* \leq \frac{86}{128}$, the process-directed self-assembly yields the metastable GYR mesostructure, which resides inside the free-energy basin of the initial, equilibrium mesophase. As f_A^* increases, however, the size of this GYR basin decreases. For $f_A^* \geq \frac{87}{128}$, eventually, the alchemical conversion process catapults the starting, unstable state out of the GYR free-energy basin (which still exists because of the metastable GYR mesostructure) into the DIA free-energy basin. The subsequent, spontaneous structure formation yields the metastable DIA mesostructure.

In summary, we studied the process-directed self-assembly for fabricating metastable mesostructures using dynamic self-consistent field calculations and particle-based simulations. Illustrating the concept by an alchemical conversion process, we have systematically studied the process-accessible mesostructures at intermediate segregation as a function of the initial and final A volume fractions. In addition to the common equilibrium mesophases, the diagram of process-accessible states encompasses multiple additional mesostructures, of which some have not been reported before. Generally, we find that the sequence of final, metastable mesostructures after the alchemical conversion process coincides in symmetry with the initial, equilibrium mesophase and strongly differs from the equilibrium mesophases at the same value of f_A^*. We argue that this general trend arises from the "weakness" of the alchemical conversion process that does not catapult the starting, unstable state into a new free-energy basin. Notable exceptions are the formation of the metastable DIA and fcc* mesostructures.

Whereas our study focuses on a specific example of a rapid thermodynamic process, we expect that our qualitative observations are rather robust because they are based on the universal structure of the free-energy landscape. We hope that our predictions will stimulate experimental efforts that explore the complex free-energy landscape of these fascinating soft materials, confirm our predictions of novel

metastable mesostructures, and test our strategy to reproducibly fabricate the desired metastable mesostructures.

We acknowledge stimulating discussions with G. E. Schröder-Turk, A. H. Schoen, E. Koch, G. J. A. A. Soler-Illia, L. Schneider, W. H. Li, Y. Z. Ren, G. J. Zhang, and Q. Y. Tang. Financial support was provided by the Deutsche Forschungsgemeinschaft under Grant No. DFG Mu1674/14-1. Simulations were performed at GWDG Göttingen, HLRN Hannover/Berlin, and JSC Jülich, Germany.

*mmueller@theorie.physik.uni-goettingen.de

[1] F. S. Bates and G. H. Fredrickson, Phys. Today No. 2, **52**, 32 (1999).
[2] F. S. Bates, Mater. Res. Bull. **30**, 525 (2005).
[3] A. J. Meuler, M. A. Hillmyer, and F. S. Bates, Macromolecules **42**, 7221 (2009).
[4] M. W. Matsen and F. S. Bates, Macromolecules **29**, 1091 (1996).
[5] cps either refers to face-centered-cubic spheres (fcc) or hexagonally close-packed spheres (HCP).
[6] M. W. Matsen and M. Schick, Phys. Rev. Lett. **72**, 2660 (1994).
[7] C. A. Tyler and D. C. Morse, Phys. Rev. Lett. **94**, 208302 (2005).
[8] M. W. Matsen, Eur. Phys. J. E **30**, 361 (2009).
[9] W. H. Li and M. Müller, Prog. Polym. Sci. **54–55**, 47 (2016).
[10] C.-Z. Zhang and Z.-G. Wang, Phys. Rev. E **73**, 031804 (2006).
[11] U. Nagpal, M. Müller, P. F. Nealey, and J. J. de Pablo, ACS Macro Lett. **1**, 418 (2012).
[12] W. H. Li and M. Müller, Annu. Rev. Chem. Biomol. Eng. **6**, 187 (2015).
[13] F. Drolet and G. H. Fredrickson, Phys. Rev. Lett. **83**, 4317 (1999).
[14] Y. Bohbot-Raviv and Z.-G. Wang, Phys. Rev. Lett. **85**, 3428 (2000).
[15] Z. Guo, G. Zhang, F. Qiu, H. Zhang, Y. Yang, and A. C. Shi, Phys. Rev. Lett. **101**, 028301 (2008).
[16] A. Ranjan, J. Qin, and D. C. Morse, Macromolecules **41**, 942 (2008).
[17] W. Q. Xu, K. Jiang, P. W. Zhang, and A. C. Shi, J. Phys. Chem. B **117**, 5296 (2013).
[18] C. L. Tsai, K. T. Delaney, and G. H. Fredrickson, Macromolecules **49**, 6558 (2016).
[19] X. Cheng, L. Lin, W. E, P. Zhang, and A. C. Shi, Phys. Rev. Lett. **104**, 148301 (2010).
[20] M. Müller and D.-W. Sun, Phys. Rev. Lett. **111**, 267801 (2013).
[21] M. Müller and D.-W. Sun, J. Phys. Condens. Matter **27**, 194101 (2015).
[22] For instance, a spiropyran group can exhibit photoreversible hydrophilicity change between closed-ring and open-ring forms [23]. Another photoreversible example is the light-induced trans ⇌ cis isomerization of the azobenzene [24] that can significantly change the dipole moment. Additionally, since the alchemical transformation does not need to be photoreversible, photolabile protecting groups ("cages") can also be employed to induce light-triggered changes in hydrophilicity, e.g., by photocleavage of NVOC groups [25].
[23] J. Zhang, Y. Zhang, F. Y. Chen, W. Y. Zhang, and H. Y. Zhao, Phys. Chem. Chem. Phys. **17**, 12215 (2015).
[24] D. Huebner, C. Rossner, and P. Vana, Polymer **107**, 503 (2016).
[25] A. Brunsen, J. X. Cui, M. Ceolín, A. del Campo, G. J. A. A. Soler-Illia, and O. Azzaroni, Chem. Commun. (Cambridge) **48**, 1422 (2012).
[26] J. G. E. M. Fraaije, B. A. C. van Vlimmeren, N. M. Maurits, M. Postma, O. A. Evers, C. Hoffmann, P. Altevogt, and G. Goldbeck-Wood, J. Chem. Phys. **106**, 4260 (1997).
[27] N. M. Maurits and J. G. E. M. Fraaije, J. Chem. Phys. **107**, 5879 (1997).
[28] T. Kawakatsu, Phys. Rev. E **56**, 3240 (1997).
[29] E. Reister, M. Müller, and K. Binder, Phys. Rev. E **64**, 041804 (2001).
[30] K. S. Lyakhova, A. V. Zvelindovsky, and G. J. A. Sevink, Macromolecules **39**, 3024 (2006).
[31] M. Müller and J. J. de Pablo, Annu. Rev. Mater. Res. **43**, 1 (2013).
[32] D. J. Grzetic, R. A. Wickham, and A. C. Shi, J. Chem. Phys. **140**, 244907 (2014).
[33] M. W. Matsen, J. Phys. Condens. Matter **14**, R21 (2002).
[34] M. Müller and F. Schmid, Adv. Polym. Sci. **185**, 1 (2005).
[35] G. H. Fredrickson, *The Equilibrium Theory of Inhomogeneous Polymers* (Oxford University Press, Oxford, 2006).
[36] M. Doi and S. F. Edwards, *The Theory of Polymer Dynamics* (Oxford University Press, Oxford, 2001).
[37] K. C. Daoulas and M. Müller, J. Chem. Phys. **125**, 184904 (2006).
[38] K. C. Daoulas, M. Müller, J. J. de Pablo, P. F. Nealey, and G. D. Smith, Soft Matter **2**, 573 (2006).
[39] M. Müller and K. C. Daoulas, J. Chem. Phys. **128**, 024903 (2008).
[40] M. Müller, J. Stat. Phys. **145**, 967 (2011).
[41] The starting, unstable state for $f_A^* < f_A$ can be similarly fabricated by converting an *AAB* copolymer into an *ABB* copolymer.
[42] P. C. Hohenberg and B. I. Halperin, Rev. Mod. Phys. **49**, 435 (1977).
[43] See Supplemental Material at http://link.aps.org/supplemental/10.1103/PhysRevLett.118.067801 for details of the employed theoretical methods and their numerical implementations, illustrations of the kinetics of process-directed self-assembly resulting in the metastable I-WP and hex2* mesostructures, respectively, and a discussion of the free-energy landscape in the vicinity of the metastable fcc* mesostructure, which includes Refs. [44–49].
[44] K. Ø. Rasmussen and G. Kalosakas, J. Polym. Sci. B **40**, 1777 (2002).
[45] G. Tzeremes, K. Ø. Rasmussen, T. Lookman, and A. Saxena, Phys. Rev. E **65**, 041806 (2002).
[46] M. Laradji, A. C. Shi, J. Noolandi, and R. C. Desai, Macromolecules **30**, 3242 (1997).
[47] M. Müller, Y. G. Smirnova, G. Marelli, M. Fuhrmans, and A. C. Shi, Phys. Rev. Lett. **108**, 228103 (2012).
[48] L. Leibler, Macromolecules **13**, 1602 (1980).

[49] H. D. Ceniceros and G. H. Fredrickson, Multiscale Model. Simul. **2**, 452 (2004).
[50] Here, we only consider process-directed self-assembly that starts from spatially modulated, equilibrium mesophases. One could also start from the disordered phase with thermal fluctuations. The concomitant spinodal self-assembly presumably results often in the formation of the equilibrium mesophases at f_A^*.
[51] We only consider the fcc arrangement but not the HCP arrangement of close-packed spherical domains.
[52] A. H. Schoen, NASA Technical Note No. TN D-5541, 1970, http://ntrs.nasa.gov/archive/nasa/casi.ntrs.nasa.gov/19700020472_1970020472.pdf.
[53] E. A. Lord and A. L. Mackay, Curr. Sci. **85**, 346 (2003).
[54] G. E. Schröder-Turk, A. Fogden, and S. T. Hyde, Eur. Phys. J. B **59**, 115 (2007).
[55] K. Jiang, C. Wang, Y. Q. Huang, and P. W. Zhang, Commun. Comput. Phys. **14**, 443 (2013).
[56] Y. Gao, H. Deng, W. Li, F. Qiu, and A. C. Shi, Phys. Rev. Lett. **116**, 068304 (2016).
[57] The metastable Schoen's F-RD mesostructure can be obtained by joining the enlarged face-centered-cubic *A* spheres between the first nearest neighbors. We employ the notations, F-RD and I-WP, according to Ref. [52].
[58] If we make the connectors in GYR and DIA mesostructures, respectively, become thinner and thinner and finally broken, the spherical domains left result in the formation of GYR-S and DIA-S mesostructures, respectively. We use the notations, I-WP-S, GYR-S, and DIA-S, to label these three metastable spherical mesostructures because the three changes, I-WP-S $\rightleftharpoons$ I-WP, GYR-S $\rightleftharpoons$ GYR, and DIA-S $\rightleftharpoons$ DIA, are all completely gradual.